

Journal of Materials Chemistry B

Accepted Manuscript



This is an *Accepted Manuscript*, which has been through the Royal Society of Chemistry peer review process and has been accepted for publication.

Accepted Manuscripts are published online shortly after acceptance, before technical editing, formatting and proof reading. Using this free service, authors can make their results available to the community, in citable form, before we publish the edited article. We will replace this *Accepted Manuscript* with the edited and formatted *Advance Article* as soon as it is available.

You can find more information about *Accepted Manuscripts* in the [Information for Authors](#).

Please note that technical editing may introduce minor changes to the text and/or graphics, which may alter content. The journal's standard [Terms & Conditions](#) and the [Ethical guidelines](#) still apply. In no event shall the Royal Society of Chemistry be held responsible for any errors or omissions in this *Accepted Manuscript* or any consequences arising from the use of any information it contains.

Application of Layer-By-Layer Coatings to Tissue Scaffolds – Development of an Angiogenic Biomaterial

Cite this: DOI: 10.1039/x0xx00000x

C.D. Easton^a, A.J. Bullock^b, G. Gigliobianco^b, S.L. McArthur^c, S. MacNeil^{b*}

Received 00th January 2012,
Accepted 00th January 2012

DOI: 10.1039/x0xx00000x

www.rsc.org/

Tissue engineered materials aimed at wound care typically underperform due to poor engrafting to the wound bed. The need for such materials will continue to intensify as a result of an ageing population and an increase in patients suffering from vascular problems. Here we describe the development of an angiogenic coating strategy employing a combination of plasma phase deposition of acrylic acid and layer-by-layer (LBL) chemistry using polyethyleneimine and poly(acrylic acid) for the immobilization of heparin and Vascular Endothelial Growth Factor (VEGF). The formation of the coating and its ability to immobilize heparin was examined by Quartz Crystal Microbalance with Dissipation. X-ray Photoelectron Spectroscopy (XPS) and Atomic Force Microscopy were used to confirm that these coatings retained a significant amount of heparin on the surface when applied to a flat substrate. The coating strategy was transferred to 2 different tissue scaffold architectures: a commercially available non-biodegradable polypropylene mesh, and a biodegradable electrospun poly(lactico-glycolic acid) (PLGA) scaffold. XPS confirmed that the coating was successfully applied to the scaffolds and that a similar amount of heparin was immobilized. *In vitro* testing showed that while HDMEC readily attached to the PLGA scaffold, they were inhibited from adhering and forming proliferative colonies where heparin alone was attached to the LBL coated PLGA scaffold. However, after dip coating with VEGF, the heparin coated scaffold supported both attachment and colony growth of HDMEC; no such colony formation occurred in the absence of VEGF.

Introduction,

Development of flexible coating strategies to promote angiogenesis is critical to effectively treat chronic, non-healing wounds. This need will continue to grow globally in light of an ageing population and an increasing number of patients diagnosed with diabetes. In addition, such strategies are required within the tissue engineering community to overcome issues associated with engineered materials, which fail to engraft as a result of inefficient neovascularisation.

An important requirement for an angiogenic biomaterial is the ability to maintain a regulated release of bioactive growth factors to the wound site. While there are a variety of different growth factors available, it is believed that vascular endothelial growth factor (VEGF) alone is sufficient to promote angiogenesis.¹ Recently we reported an approach to produce hydrogels containing lysine and arginine to electrostatically bind heparin – which then bound VEGF – and was then demonstrated to be mitogenic for human dermal microvascular endothelial cells (HDMEC).² Heparin has been included within

scaffold architectures as a means to bind and stabilise VEGF, while regulating the release of the growth factor to promote vasculogenesis.^{3,4} A number of strategies for the use of natural and synthetic heparin-mimetics have been developed, for example heparin-loaded hydrogels,⁵⁻⁷ heparin modified tissue scaffolds,^{8,9} heparin modified bone cements,¹⁰ collagen matrices,¹¹ and functionalised micro- and nano-particles.¹²⁻¹⁴ Some wound beds can be relatively large, for example, in the case of patients with extensive full thickness burns and extensive areas of biomaterials are necessary. Moreover, there are issues with many scaffolds failing to promote angiogenesis; heparin is rapidly lost from the wound site and consequently blood vessel formation within new scaffolds can be too slow to ensure survival of the cells in the scaffold.¹⁵ Therefore, there is an increasing research effort directed towards the development of new strategies to effectively immobilise heparin for the sustained release of bioactive growth factors. Layer-by-layer (LBL) chemistry is a dip-coat strategy where multilayers comprising of consecutive layers of polyanions and polycations are physically adsorbed onto a substrate.¹⁶ LBL is a useful

methodology within the biomaterials field as it enables film growth on virtually any substrate (assuming the adsorption of the first layer is successful) regardless of its size or shape. LBL is ideal for the immobilisation of biomolecules due to electrostatic attraction between successive layers bearing opposite charge, resulting in a very compact and stable multilayer structure.¹⁷ LBL coatings have been fabricated employing either heparin,¹⁸⁻²² or heparin plus a growth factor as the polyanion;²³ however one would consider that this is not a practical use of heparin, as the majority would be located within the bulk of the coating rather than on the surface where it is required to exert biological activity.

In this study, a LBL coating strategy was developed using two polymers: poly(acrylic acid) as the polyanion and polyethyleneimine (PEI) as the polycation; a plasma polymer of acrylic acid was employed as the base layer. The formation of these coatings and their ability to bind heparin has been examined using Quartz Crystal Microbalance with Dissipation (QCM-D), X-ray Photoelectron Spectroscopy (XPS), and Atomic Force Microscopy (AFM). This methodology was then transferred onto two different scaffold types, a commercially available non-biodegradable polypropylene mesh currently used clinically in hernia repair and pelvic organ prolapsed repair,^{24, 25} and a biodegradable electrospun poly(lactic/glycolic acid) (PLGA 75:25) scaffold under development for dermal replacement.²⁶ The *in vitro* response of the coated scaffolds was investigated by examining the ability of HDMEC cells to attach and proliferate on the scaffolds.

Experimental

Plasma phase deposition. Plasma phase deposition was performed in a custom built T-shaped stainless steel reactor with stainless steel end plates sealed with Viton O-rings detailed previously.²⁷ Acrylic acid (99.5 % purity, Acros organics, USA) was degassed by at least three freeze-pump-thaw cycles prior to use. Flow rate of the monomer was controlled using a needle valve and the plasma unit pressure monitored using a Pirani gauge. A plasma phase was ignited within the reactor using a 13.56 MHz generator coupled to a stainless steel internal disc electrode via a matching network. Plasma polymers were deposited onto Si wafer (orientation <100>; thickness 600-650 μm ; single side polished; resistivity 14.0-22.0 $\Omega\cdot\text{cm}$; Micro Materials & Research Consumables, Australia), QCM crystals (QSX301 gold coated quartz (100 nm Au), Q-Sense, Sweden), polypropylene tissue scaffold (Gynecare Gynemesh* PS GPSXL3), and electrospun PLGA (75:25) tissue scaffold (Fabrication methodology reported elsewhere).²⁶ Si wafers were ultrasonically cleaned with isopropyl alcohol (Chem-Supply Pty Ltd, Australia) and dried with a stream of nitrogen gas prior to use. QCM crystals were cleaned in a solution of 5:1:1 Milli-Q water, ammonia (30% purity, Sigma-Aldrich, Australia) and hydrogen peroxide (30% purity, Riedel-de Haen, Germany) and heated to 75°C for approximately 10 minutes. Crystals were then rinsed with Milli-Q water and isopropyl alcohol, and dried with nitrogen gas. Sensors were then plasma etched with air at 50 W for 5 minutes, and wet cleaned again following the protocol described above. Tissue scaffolds were cleaned employing the same plasma etching methodology. After loading the substrates into the reactor, the unit was evacuated down to base pressure (1×10^{-3} mbar). An operating pressure of 2×10^{-2} mbar was maintained at the defined monomer flow rates by throttling the valve between the single stage rotary vacuum pump and the plasma unit. Monomer flow rate was determined using the technique outlined by Griesser and Gengenbach.²⁸ Once a stable flow rate was achieved, the plasma was

ignited for 20 min. After deposition, monomer flow was maintained for another 5 min to quench any radicals on the surface of the plasma polymers. The monomer valve was then closed and the plasma unit evacuated for approximately 5 min to remove any residual monomer from the system.

LBL fabrication and heparin absorption. Polyelectrolytes (PE) solutions of 0.5% w/v of polyethyleneimine (PEI) (Mw = 750000 g/mol; 50% w/v; Sigma Aldrich) and poly(acrylic acid) (PAC) (Mw = 100000 g/mol; 35% w/v; Sigma Aldrich) were diluted into phosphate buffered saline (PBS) (150 mM) and pH adjusted as required. For samples fabricated for XPS, AFM, or for the *in vitro* study, LBL formation was carried out on samples within 12 well tissue culture plates. 3 ml of PE solution was transferred into wells. After incubation for 30 min at RT, the solution was removed and the wells were rinsed 5 times with PBS prior to the addition of the next PE solution. This process was repeated until the desired number of layers was achieved. For QCM-D crystals, PE and PBS wash solutions were pumped through each channel at a rate of 100 $\mu\text{l}/\text{min}$ for 30 min and 5 min respectively; thus the QCM-D crystals were exposed to the same amount of PE solution as those fabricated for XPS and AFM.

For heparin absorption experiments, solutions of 1 mg/ml of heparin (heparin sodium salt from porcine intestinal mucosa, Sigma Aldrich) in PBS (150 mM) were used. Samples were incubated in 1 ml of solution for 30 min, equating to a flow rate of 33.3 $\mu\text{l}/\text{min}$ for QCM-D. After incubation, samples were rinsed with PBS, again 5 times for AFM and XPS samples in wells, while the QCM-D channels were rinsed for 20 min. AFM and XPS samples were rinsed a further 5 times with Milli-Q water (18.2 M $\Omega\cdot\text{cm}$) to remove any excess salt from the surface and then dried with nitrogen gas before analysis.

QCM-D analysis. The formation of the LBL system and absorption of heparin was studied *in situ* by Quartz Crystal Microbalance with Dissipation (QCM-D) (E4 Biolin Scientific / Q-Sense, Sweden). QCM-D E4 uses quartz crystals with a diameter of 14 mm (surface area is 153.9 mm²) and a resonant frequency 5 MHz. A detailed description of the QCM-D technique was published by Rodahl et al. [29]. QCM-D E4 contains four independent chambers thus allowing for duplicates of the experiments to be carried out simultaneously. All measurements were performed in a temperature-controlled flow chamber at 22 ± 0.05 °C.

XPS analysis. X-ray photoelectron spectroscopy (XPS) analysis was performed using an AXIS Ultra DLD spectrometer (Kratos Analytical Inc., Manchester, UK) with a monochromated Al K α source at a power of 150 W (15 kV \times 10 mA), a hemispherical analyser operating in the fixed analyser transmission mode and the standard aperture (analysis area: 0.3 mm \times 0.7 mm). The total pressure in the main vacuum chamber during analysis was less than 10^{-8} mbar. Survey spectra were acquired at a pass energy of 160 eV. To obtain more detailed information about chemical structure, oxidation states etc., high resolution spectra were recorded from individual peaks at 40 eV pass energy (yielding a typical peak width for polymers of 1.0 – 1.1 eV). Each specimen was analysed at an emission angle of 0° as measured from the surface normal. Assuming typical values for the electron attenuation length of relevant photoelectrons the XPS analysis depth (from which 95% of the detected signal originates) ranges between 5 and 10 nm. Data processing was performed using CasaXPS processing software version 2.3.15 (Casa Software Ltd., Teignmouth, UK). All elements present were identified from survey spectra. The atomic concentrations of the detected elements were calculated using integral peak intensities and the sensitivity factors supplied by the manufacturer. Binding energies were referenced to the aliphatic hydrocarbon peak at 285.0 eV. The accuracy associated with

quantitative XPS is ca. 10% - 15%. Precision (i.e. reproducibility) depends on the signal/noise ratio but is usually much better than 5%. The latter is relevant when comparing similar samples.

Atomic Force Microscopy. An Asylum Research MFP-3D atomic force microscope (Santa Barbara, CA, USA) was used to measure surface topography in tapping mode with ultra-sharp silicon nitride tips (NSC15 noncontact silicon cantilevers, MikroMasch, Spain). The tips used in this study had a typical force constant of 40 N/m and a resonant frequency of 320 kHz. Typical scan settings involved the use of an applied piezo deflection voltage of 0.6 – 0.8 V at a scan rate of 0.6 – 0.8 Hz. All images were processed (1st order flattening algorithm) using Igor Pro software.

In vitro performance of scaffolds. PLGA scaffolds were electrospun from a 10% wt/wt solution of PLGA (75:25) in dichloromethane (Fisher, UK). The solution was pumped from 4 syringes (40 μ l/s per syringe) and subjected to an accelerating voltage of 17kV, an aluminium foil coated earthed rotating collector (20cm wide, 10cm diameter, 200 RPM) was placed 17cm from the charged needle tips, 0.6g of PLGA was electrospun on to a 20x30cm sheet. PLGA scaffolds were then coated by plasma phase deposition prior to being subjected to the LBL process and were then dip-coated with heparin (1mg/ml) in PBS by incubation with gentle shaking for 24 hours and were then dip-coated with 200ng/ml VEGF (ABD Serotec, UK) in PBS, with gentle shaking at 4°C for 24 hours. All samples were washed 3 times with sterile PBS between coatings. 2 x 2cm sheets were prepared and placed in 12 well tissue culture plates.

VEGF binding to scaffolds. 0.8cm diameter discs of scaffold bearing 1, 3, 5, and 7 layers deposited by the LBL process were dip-coated with heparin (1mg/ml in dH₂O) at room temperature for 4 hours. These were then washed in PBS then dip-coated in 1 ml of 1 μ g/ml VEGF (ABD Serotec, UK) in PBS, with gentle shaking at 4°C for 10hours. After washing once with PBS, samples were then incubated in 1ml of PBS for 24 hours at room temperature before the PBS was assayed for VEGF with a Human VEGF ELISA kit from Peptide (New Jersey, USA), the assay was carried out according to manufacturer instructions. The ELISA plate was read at 405 nm (reference 630 nm), VEGF standards were used to create a calibration curve.

Direct seeding with cells. HDMEC cells (Promocell, UK) were cultured in endothelial cell (EC) growth medium (Promocell MV2, Promocell, UK) in gelatin coated tissue culture plastic T25 culture flasks.³⁰ Immediately prior to use, T25 flasks of near confluent HDMEC cells were washed 3 times with PBS, then incubated with Celltracker Red (Invitrogen, UK) (10 μ g/ml in serum free endothelial cell growth medium) for 45 minutes at 37°C. Cells were gently washed 3 times with PBS, then detached from the culture flask by treatment with trypsin-EDTA (Invitrogen, UK) (Sigma Aldrich, UK), and an appropriate dilution of cells was made in EC medium. 100,000 cells per sample were pipetted into a 1cm diameter culture well formed from a 1cm diameter steel ring placed on top of a 2 x 2 cm sheet of scaffold. Cells were allowed to adhere for 24 hours before the ring was removed, and the scaffold gently washed once with media to removed non adherent cells, and the scaffold placed into a clean culture well, and submerged in culture medium. At 48h, cells were imaged to assess the density of HDMEC cells in each scaffold. Photographs were taken of 3 fields of view at 100x magnification for each sample with an Axon ImageExpress (Molecular Devices, USA) fluorescence microscope (10x objective, λ_{ex} 577nm, λ_{em} 602nm). The number of cells visible

in each photograph was counted using the cell counter macro of ImageJ, (NIH, Maryland USA).

Transfer of HDMEC cells onto scaffolds. HDMEC cells were seeded into gelatine (Sigma, UK) coated 12 well plates at a density of 100,000 per well in media, and allowed to grow to confluence. Scaffolds were cut into 2cm x 0.5cm strips and fixed into 12 well sized Scaffoldex frames (Scaffoldex, Tampere, Finland). These were placed in the culture wells such that the scaffolds were held against the layer of cells at the base of the well, facilitating migration of HDMECs adhered to gelatine to the fibres of the scaffold - simulating in vivo in migration. After 48h, the scaffolds were removed and cell attachment to the scaffolds was assessed. Photographs were taken with an Axon ImageExpress fluorescence microscope (100x magnification, 10x objective, λ_{ex} 577nm, λ_{em} 602nm).

Results

3.1 Examining the formation of the LBL coating – QCM-D.

A key requirement when developing a coating strategy for use in wound care is having the flexibility to apply it to a variety of substrates; this is due to the assortment of scaffold types commercially available and the continual emergence of new scaffold architectures. For a coating strategy based on LBL chemistry, the surface charge of the substrate is critical, as the first layer must physically absorb and be stable. To overcome the variance in surface charge between the various substrate types, a surface pre-treatment should be undertaken. From the available methods, plasma phase deposition was employed to deposit onto the substrate a uniform coating of known surface charge, specifically a negative surface charge employing acrylic acid. Plasma phase deposition was chosen as it is a dry fabrication technique and the coatings can be applied to a number of substrates.³¹ Plasma polymers have often been employed within the biomaterials field to provide desirable surface properties for the intended substrate, where recently we demonstrated the use of a plasma polymer in fabricating microwells for peptide display.³² The properties of plasma polymer acrylic acid (ppAAc) deposited from the reactor used in this study, including surface charge characteristics, have been reported previously;²⁷ a typical high resolution C 1s XPS spectrum and AFM image for this thin film can be found in the supplementary information (Fig. S1).

There are a number of parameters that influence the formation of LBL coatings, including: polymer type and concentration, salt concentration, and pH. For this particular application, ideally both PEs should be inexpensive, well defined, easy to deploy and non-cytotoxic. To satisfy these requirements, poly(acrylic acid) (PAC) and polyethyleneimine (PEI) were selected as the polyanion and polycation respectively. The examination of all the various design parameters on the resultant LBL coating properties would be outside the scope of this particular work; initial work using QCM-D demonstrated that the polymer pH employed during LBL formation had an effect on the amount of heparin adsorbed on the final coating. The system that adsorbed the most heparin within the parameter space explored was chosen for this study, specifically pH (PEI) = 9 and pH (PAC) = 4. This approach is similar to that used previously by Muller *et. al.*³³ for fabricating LBL coatings. At pH 7, the PEI would be positively charged, while the PAC would be negatively charged. At pH 4, the PAC would be weakly charged or uncharged while the PEI would be highly ionized, and vice-versa at pH 9. Note the first layer of PEI was absorbed at pH 7 rather than pH 9 to prevent the ppAAc base

layer delaminating when hydrated in a strong base (data not shown).

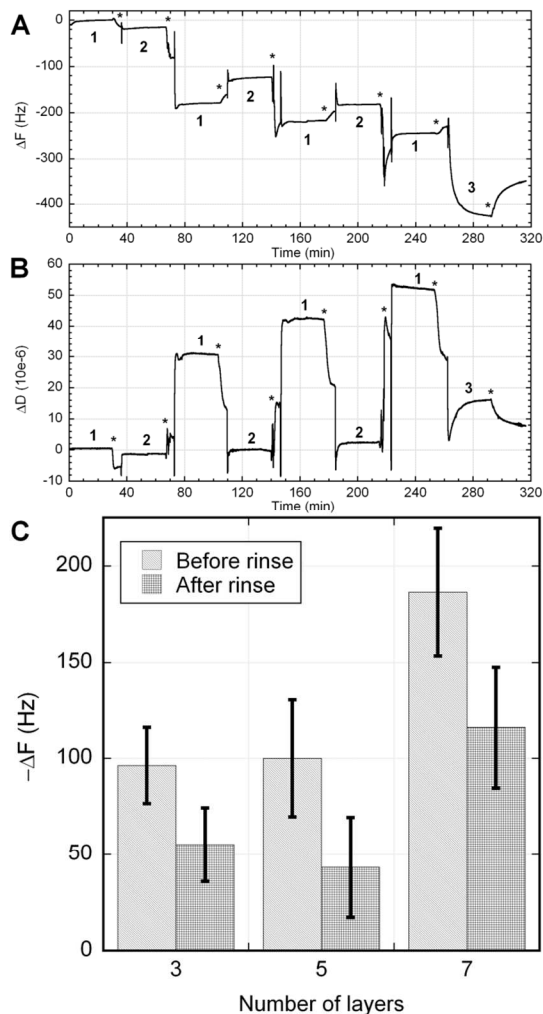


Fig. 1. (A) and (B) Selected, representative QCM-D data of 7-layer LBL system with absorption of heparin. Labels correspond to following steps: 1 – PEI; 2 – PAC; 3 – Heparin; * – PBS wash. (C) Summary of QCM-D results for heparin absorption and retention on LBL systems fabricated with 3, 5 or 7 layers. Error bars represent standard deviation derived from 4 measurements.

Selected, representative QCM-D data for the 7 layer LBL system with heparin subsequently absorbed is presented in Fig. 1A and 1B. Each physical adsorption step is followed by a PBS rinse (at pH 7.4). As a decrease in ΔF represents mass added to the system, while an increase in ΔD indicates an increase in viscoelasticity (i.e. the adsorbing layers swell and hold water, effectively softening the interface and damping the crystal oscillation), the QCM data confirms the formation of the LBL system. The general trend is that each subsequent adsorption step results in mass added, and in a more viscoelastic (softer) film. Once the system exceeds 4 layers, another trend can be observed where the addition of the polyanion results in what appears to be a loss in mass, causing an oscillation in ΔF and ΔD with the addition of each subsequent layer. Similar trends have been observed previously for both ΔF and ΔD and have been attributed to swelling-and-shrinking of the outermost PE layer, or redissolution and/or rearrangement of PE complexes.^{34, 35}

Addition of heparin to the system resulted in a significant increase in mass added; rinsing with PBS led to a decrease in mass associated with partial removal of heparin; however the total mass of the system was still greater than before heparin absorption. Interestingly, after addition of heparin and rinsing with PBS, a significant decrease is observed for ΔD , indicating that the system has collapsed, excluding water from the film and creating a rigid layer.

A summary of the QCM-D ΔF results are presented in Fig. 1C, where the ΔF values presented are the difference in the ΔF immediately before heparin addition, and either before or after the final PBS rinse. LBL systems with 3, 5, and 7 layers were used for the immobilization of heparin. In all cases it is observed that rinsing with PBS partially removed heparin from the system; 3 and 5 layer LBL coatings resulted in approximately the same amount of heparin absorption and retention, while the 7 layer system resulted in a greater amount of heparin retention.

3.2 Examining the resultant LBL coating - XPS and AFM.

The plasma phase deposition/LBL methodology was transferred to Si wafer to examine the surface chemistry and topography. The elemental composition obtained via XPS is presented in Table 1 while selected, representative high resolution C 1s spectra are shown in Fig. 2. From the survey data it is clear that heparin was not present on the ppAAc coating after incubation as no S signal was detected. Within the XPS sampling depth (< 10 nm), the 5 layer (LBL 5) and 7 layer (LBL 7) systems were approximately the same in both elemental composition and from the high res C 1s data (Fig. 2A); this was somewhat unexpected. Once heparin was absorbed, both were very similar though the 7 layer system appeared to have slightly more heparin present (S content – 2.8 % vs. 3.0 %) confirming QCM-D observations.

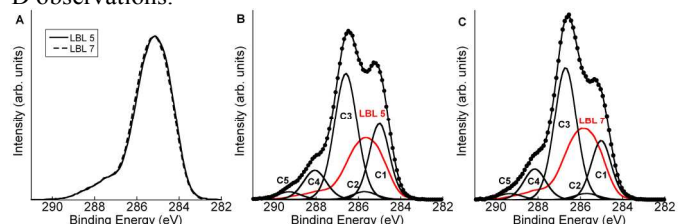


Fig. 2. Selected, representative XPS high resolution C 1s spectra of LBL 5 and LBL 7 samples prepared on Si wafer, (A) LBL 5 and LBL 7 systems, (B) LBL 5 + heparin, (C) LBL 7 + heparin. Filled circles represent measured spectrum while corresponding solid line represents fit from components. Labeled components correspond to the following: C1 – C-C and C-H (hydrocarbons), C2 – secondary shift associated with acid, ester (i.e. C5); C3 – C-N, C-O based groups (ethers and alcohols); C4 – C=O and O-C-O based groups (e.g. aldehyde, ketone); C5 – O-C=O based groups (e.g. acid, ester); LBL 5 and LBL 7 – model spectra obtained experimentally.

For the 5 and 7 layer systems with heparin, the high resolution C1s spectra were fitted using a combination of standard components (Gaussian-Lorentz) and a model C 1s spectrum obtained from the corresponding LBL system (i.e. the spectra presented in Fig. 2A). This technique allows for the specific identification of changes in the C 1s profile as a result of the heparin absorption. To ensure the contribution from the underlying LBL substrate and the heparin are realistic, the ratio of C3 (C-O based groups) and C4 (O-C-O based groups) was

confirmed to be approximately equal to that of the theoretical value for heparin (i.e. C4:C3 = 2:9) during the fitting procedure, as these are the two major contributions from heparin to the carbon signal. As observed from Fig. 2B and 2C, the underlying LBL substrate has a contribution to the overall C 1s spectrum but is not the dominant component, accounting only for approximately 35% of the signal. In both cases, the ratio of C4 to C3 was as expected, with no residual discrepancy between the model fit and the measured spectrum, thus indicating a good fit.

Table 1. Atomic ratios relative to total concentration of carbon (X/C) obtained by XPS of LBL coatings on Si wafer. Listed are the mean values (\pm deviation) based on +2 analyses performed on each sample. Trace amounts of: ^aNa, ^bCl, ^cP, ^dSi.

Sample	O/C	N/C	S/C
ppAAc ^d	0.370 \pm 0.005	0.005 \pm 0.000	-
ppAAc + Hep ^{a,d}	0.344 \pm 0.002	0.005 \pm 0.001	-
LBL 5 ^{b,c,d}	0.252 \pm 0.006	0.256 \pm 0.001	0.001 \pm 0.000
LBL 5 + Hep ^{b,c,d}	0.446 \pm 0.014	0.178 \pm 0.005	0.047 \pm 0.001
LBL 7 ^{b,c,d}	0.262 \pm 0.005	0.262 \pm 0.004	-
LBL 7 + Hep ^{b,c,d}	0.463 \pm 0.016	0.185 \pm 0.005	0.051 \pm 0.002

High resolution N 1s spectra of the LBL 7 system with and without heparin were examined (see Fig. 3). The component C1 is associated with C-N groups which are present in both the PEI and heparin, while the binding energy (BE) location of C2 is indicative of charged N species. In both cases, C1 and C2 are roughly 50%. Heparin has only one N unit per unit of heparin that would contribute to C1. It would be expected that the ratio of C1 and C2 would change if heparin simply physically absorbed onto the surface, thus the data suggests the absorption process is not straightforward.

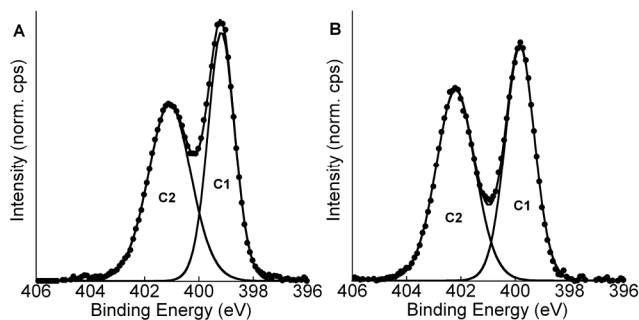


Fig. 3. Selected, representative XPS high resolution N 1s spectra of samples prepared on Si wafer, (A) LBL 7 and (B) LBL 7 + heparin. Filled circles represent measured spectrum while corresponding solid line represents fit from components. Labeled components correspond to the following: C1 – amine groups, C2 – charged N species (N⁺).

AFM images of the LBL 5 and LBL 7 systems, with and without heparin are presented in Fig. 4. LBL 5 (Fig. 4A) appears very similar to ppAAc with only PEI absorbed (See supplementary information Fig. S1B). Addition of heparin to the surface (Fig. 4B) resulted in an increase in surface roughness; however the surface structure remained generally the same. The LBL 7 system (Fig. 4C) looks very different

compared to the LBL 5 system, as it consists of very large structures protruding from a relatively smooth background. However, once heparin is included in the system (Fig. 4D), it appears very similar to the LBL 5 system + heparin (compared with Fig. 4B). It is worth noting that due to the complex and highly charged surface of the LBL 7 system containing heparin, sample imaging was very challenging and tip-surface convolution could not always be avoided.

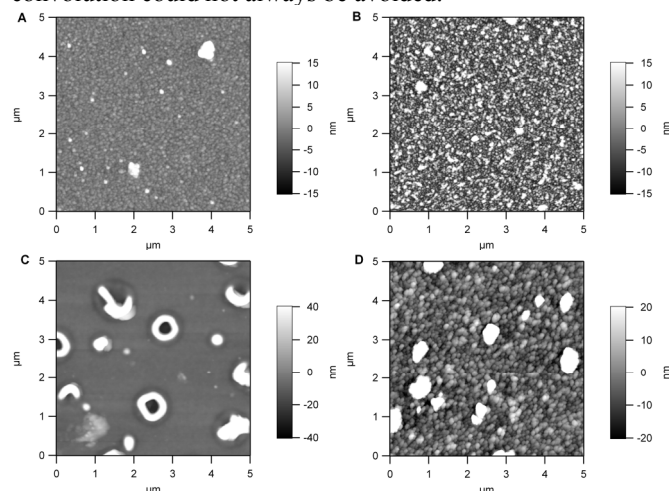


Fig. 4. Selected, representative AFM images of LBL systems prepared on Si wafer, (A) LBL 5, (B) LBL 5 + heparin, (C) LBL 7, (D) LBL 7 + heparin. Note: Due to significant surface charge, some tip-surface convolution could not always be avoided (Fig. 4D).

3.3 Transfer of LBL coating strategy to tissue scaffolds

As the proposed coating strategy was developed to promote angiogenesis for wound care applications, successful transfer of the methodology to application-relevant substrates is required. In this study, 2 different tissue scaffolds were employed: a commercially available polypropylene (PP) type and an electrospun poly(lactic-co-glycolic acid) (PLGA) (75:25) reported previously for dermal replacement.²⁶ An optical image showing a detailed view of the weave for the PP scaffold, in addition to SEM images of the PP scaffold and PLGA scaffold are shown in Fig. S2.

The fabrication process of the LBL system onto the scaffolds was examined by XPS (Table 2 and Fig. S3). The surface chemistry of the scaffolds 'as received' appeared as expected. In an attempt to clean the scaffolds prior to plasma polymer deposition, the scaffolds were plasma etched in air for 10 minutes. From the survey data (Table 2) and the high resolution C 1s spectra (Fig. S3A and S3B), the plasma etch reduced the hydrocarbon contribution and oxidized the surface of the substrates. Next, ppAAc was applied to both surfaces. Using the high resolution C 1s spectra of the plasma etched scaffolds and the ppAAc deposited on Si obtained previously, the high resolution C 1s spectra of the ppAAc treated scaffolds were fitted using components based on model spectra (Fig. S3C and S3D). For both scaffolds, it is apparent that the coating is thinner than the XPS sampling depth as a contribution from the substrate can be observed. It is difficult to conclude absolute ppAAc thickness however as the increased surface roughness of the scaffolds would mean that value for the actual emission angle is ill-defined.

The LBL 7 coating was then applied to both scaffold types (Table 2 and Fig. 5). The elemental composition of the LBL system is different for the two scaffolds, and both are different

to that obtained on Si (Table 1). On Si, O/C and N/C = 0.262; for the pp scaffold both O/C and N/C are lower (0.229 and 0.198, respectively), while for the PLGA scaffold only O/C was higher (0.310) while N/C is approximately the same (0.260). To gain a better understanding of the significance of the differences, the oxygen content relative to nitrogen (O/N) was also examined. While O/N ~ 1 for the coating on Si, O/N ~ 1.1 for the coating on both scaffold types. Overall, it appears that besides a different amount of carbon, LBL coatings displayed more oxygen than nitrogen when deposited onto the scaffolds, as opposed to deposition on a Si wafer. Small differences in composition were also reflected in the high resolution C 1s data (Fig. 5A), however they share a similar spectra profile to the LBL 7 on Si (Fig. 2A). Once heparin was absorbed to the LBL system on both scaffolds, similar amounts of S were observed compared to that obtained on the system with Si substrate (S/C of 0.051 on Si vs. 0.051 on PP vs. 0.055 on PLGA); high resolution C 1s profiles for both scaffolds with LBL 7 + heparin also presented similar profiles to that of the system on Si (Fig. 2C compared to Fig. 5B and 5C) as the bulk of the carbon signal was dominated by species associated with heparin.

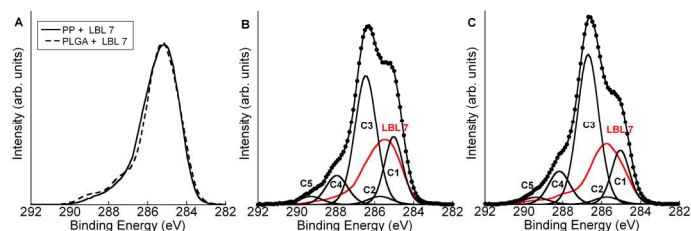


Fig. 5. Selected, representative XPS high resolution C 1s spectra of samples prepared on tissue scaffolds, (A) PP + LBL 7 and PLGA + LBL 7, (B) PP + LBL 7 + heparin, (C) PLGA + LBL 7 + heparin. Labeled components correspond to the following: C1 – C-C and C-H (hydrocarbons), C2 – secondary shift associated with acid, ester (i.e. C5); C3 – C-N, C-O based groups (ethers and alcohols); C4 – C=O and O-C-O based groups (e.g. aldehyde, ketone); C5 – O-C=O based groups (e.g. acid, ester); LBL 7 – model spectrum obtained experimentally.

3.4 *In vitro* response of LBL coated scaffolds

The data presented in Figure 6 shows that where 3, 5, or 7 layers of LBL are coated with heparin (shown to be similar between the 3 groups via QCM-D (Fig 1C)) the amount of VEGF bound was also similar.

Direct seeding of HDMEC cells onto uncoated PLGA scaffolds and LBL 7 coated PLGA scaffolds resulted in moderate cell adhesion (Fig. 7A – 7D). Cells were evenly distributed over the upper surface of the scaffolds 48 h after seeding with no visible difference in the degree of cell attachment between the two sets of scaffolds. Cellular morphology shows cells adhering tightly to fibres and spreading along the body of the fibres. In places there were small clusters of cells (Fig. 7A and 7B).

Addition of heparin to the LBL 7 coated scaffold led to a significant reduction in the number of cells attached 48 h post seeding, with cells being much more sparse than on uncoated or LBL 7 coated scaffolds and cellular morphology was rounded with little or no evidence of spreading along the fibres (Fig. 7C). The addition of VEGF to the LBL 7 + heparin scaffold significantly increased the number of cells present on the scaffold compared to both the uncoated and heparin coated scaffolds. Both sparse single cells and larger clusters of proliferating cells were apparent on these scaffolds. The

clusters of cells on the VEGF treated scaffolds were larger than those seen on any other scaffold assessed (Fig. 7D). Figure 8 shows a summary of cell density measured by counting the number of DAPI stained cell nuclei of cells attached after 48hours of incubation in 3 fields of view per sample.

Table 2. Atomic ratios relative to total concentration of carbon (X/C) obtained by XPS of LBL coatings on tissue scaffolds. Listed are the mean values (\pm deviation) based on +2 analyses performed on each sample. Trace amounts of: ^a Na, ^b Cl, ^c P, ^d Si, ^e Ca, ^f P.

Sample	O/C	N/C	S/C
PP ^{d,e}	0.029 \pm 0.005	0.002 \pm 0.002	0.001 \pm 0.000
PLGA ^{a,d}	0.488 \pm 0.009	0.000 \pm 0.000	0.000 \pm 0.000
Plasma etched PP ^{a,d}	0.242 \pm 0.006	0.078 \pm 0.002	0.004 \pm 0.001
Plasma etched PLGA ^d	0.656 \pm 0.014	0.061 \pm 0.001	0.000 \pm 0.000
PP + ppAAc ^{d,e}	0.339 \pm 0.007	0.001 \pm 0.001	0.003 \pm 0.000
PLGA + ppAAc ^d	0.413 \pm 0.004	0.004 \pm 0.001	0.000 \pm 0.000
PP + LBL 7 ^{b,d,f}	0.229 \pm 0.006	0.198 \pm 0.004	0.004 \pm 0.001
PLGA + LBL 7 ^{b,d,f}	0.310 \pm 0.001	0.260 \pm 0.001	0.000 \pm 0.000
PP + LBL 7 + hep ^{a,c}	0.446 \pm 0.011	0.162 \pm 0.009	0.051 \pm 0.002
PLGA + LBL 7 + hep ^d	0.519 \pm 0.015	0.187 \pm 0.001	0.055 \pm 0.000

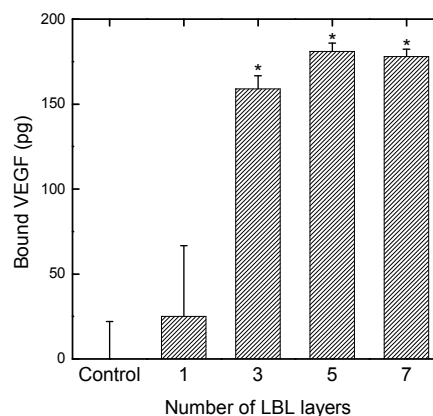


Fig. 6. VEGF binding to 8mm diameter scaffold discs dip-coated with heparin attached to increasing numbers of LBL layers. Values are mean values SEM, n=3 Statistical significance by paired T test * = P<0.05.

When scaffolds were placed in contact with confluent sheets of HDMEC cells grown on gelatin coated tissue culture plastic, it was possible to detect transfer of cells from the sheets of cells to the scaffolds. Transfer of Celltracker Red stained cells from the gelatin coated plastic was successful to varying degrees for all of the scaffolds (Fig. 7E – 7H). The uncoated and LBL 7

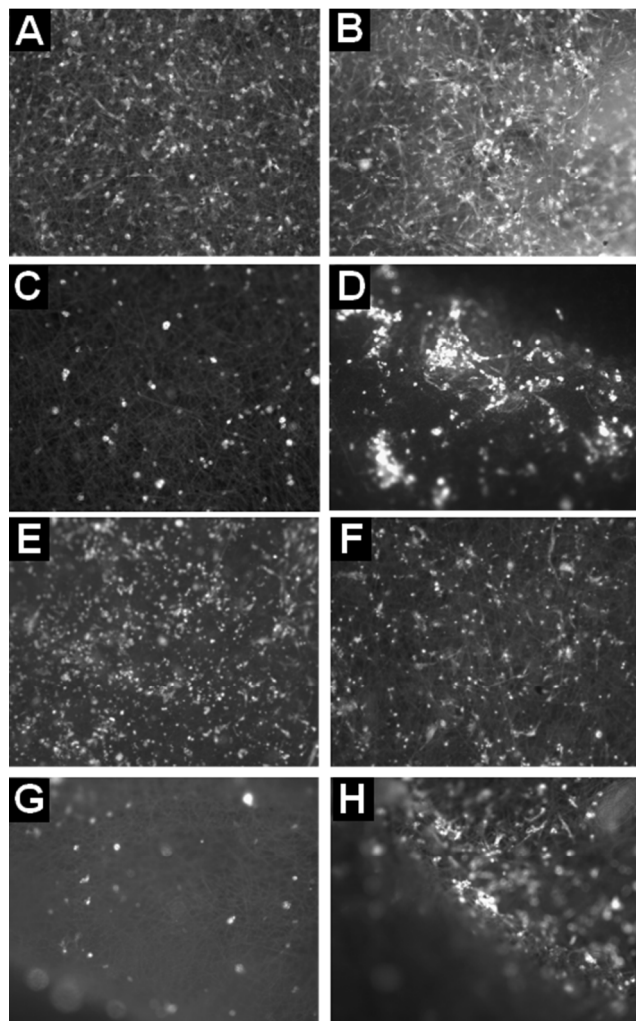


Fig. 7. DAPI stained HDMEC cells seeded onto dip-coated electrospun PLGA fibres (A – D), (A) PLGA, (B) PLGA + LBL 7, (C) PLGA + LBL 7 + heparin, (D) PLGA + LBL 7 + heparin + VEGF. DAPI stained HDMEC cells transferred onto dip-coated electrospun PLA fibres after 48h in contact with confluent HDMEC, (E) PLGA, (F) PLGA + LBL 7, (G) PLGA + LBL 7 + heparin, (H) PLGA + LBL 7 + heparin + VEGF.

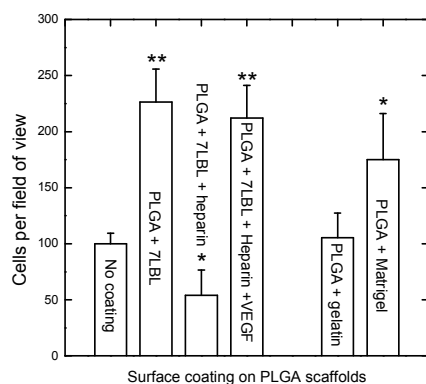


Fig. 8. Cell binding to dip-coated electrospun PLGA fibres after 48hours of incubation. Control is PLGA alone, PLGA + LBL 7, PLGA + LBL 7 + heparin, PLGA + LBL 7 + Heparin +VEGF, PLGA + gelatin, and PLGA + Matrigel. Data is the

mean + the SEM, n=3. Statistical significance by paired T test, * = $P < 0.10$, ** = $P < 0.05$.

coated scaffolds had cells attached where the scaffold was maintained in contact with the sheet of HDMEC cells. Cells were evenly distributed and appeared to have a normal morphology (Fig. 7E and 7F). Addition of heparin to the LBL7 scaffold reduced this transfer, with a marked reduction in the number of cells, and these cells had a more rounded appearance (Fig. 7G). Inclusion of VEGF on the LBL 7 + heparin coated scaffold increased the number of cells and appeared to promote small colony formation similar to that seen in direct seeding experiments (Fig. 7H).

Discussion

LBL chemistry is a well-established coating methodology and as such there is a very large body of knowledge available regarding its fabrication. While there are works published that employ PEI as a cation and others where PAC has been used as an anion, there are only a few papers where both have been employed in conjunction to create a multilayer film structure.^{33, 36, 37} Recently PEI- Ag^+ and PAC, together with silane chemistry was used to create free standing films.³⁸ Considering that the pH of the PE is switched between layers during the fabrication process, the ionization of the existing top layer is therefore not constant. While work has been done to understand the effect of ionization on the LBL formation, such as that by Caruso *et al.*,³⁹ typically in the systems explored the ionization of only one of the polymers is adjustable, not of both. The direct result of the pH switching on the QCM behavior can be observed in the transitions between PEs and rinsing stages, as there are now multiple oscillations in the measured signal rather than a single, smooth transition (i.e. Fig. 1A and 1B).

Before rinsing, an oscillation in both ΔF , and ΔD is observed, with mass load and viscoelastic increase occurring on the PEI step, respectively. When PEI is the top layer it, swells comparatively more than PAC. Once the channel is rinsed, the trends in the QCM data became less clear. However, overall it appears that when PEI is the top layer, rinsing removes a small amount of the absorbed layer, most likely in the form of PE complexes. When PAC is the top layer, rinsing appears to cause the layer to swell, likely as a result of the change in ionisation, as observed by the mass added and increase in viscoelasticity of the system. These pH dependent structural changes observed would most likely result in intercalation of the PEs between the layers.

Considering the XPS elemental composition of the LBL 5 and LBL 7 systems, the ~ 1:1 ratio of N:O would indicate that we see two PEI units for each PAC unit; however, the high resolution C 1s spectrum would suggest otherwise. The bulk of the C 1s signal (Figure 2A) is likely associated with two components, one assigned to contributions from hydrocarbons and the other to C-N. If we consider the overall peak shape, including symmetry and intensity, it appears that the contribution from C-N is larger and broader than expected, and also shifted to higher along the BE scale than is typical. In addition, the contribution at higher binding energies (~ 289 eV), typically associated with acrylic acid groups from PAC/ppAAc appears to be minor. There are likely two unique contributions that are causing this observed discrepancy between the elemental composition and the high resolution C 1s spectrum. Firstly, it is likely there is another source of O in the form of C-O that is adding to both the measured O content and the

intensity of the C 1s peak at around 286 eV. In addition, the spherical agglomerates observed via AFM would suggest the formation of PE complexes. This has been observed previously for LBL systems that include PEI.³⁴ The formation of complexes would result in a shift in the C 1s contributions originating from acrylic acid to lower binding energy and the contributions from C-N to higher binding energy as a result of the charge interaction. The high resolution N 1s spectra (Figure 3A) provide further evidence for this with the presence of the peak at higher BE associated with charged N species.

Schematic representations of LBL coatings typically present a system where the layers are intermixed, rather than discrete as a result of the layer formation processes. Thus the XPS results for the LBL coating on Si were somewhat unexpected, as both the LBL 5 and LBL 7 systems are very similar. While in both cases the top layer is PEI, you would expect the surface chemistry to differentiate somewhat as layer formation (e.g. thickness growth) is typically nonlinear. In addition, the location of the cationic and anionic groups on the polymer backbone of the PEs should lead to increased inter-diffusion of the layers.⁴⁰ This result suggests that by 5 layers, the layer formation process is chemically similar from a surface perspective to surfaces containing a greater number of layers while under vacuum.

Once heparin was absorbed onto the LBL systems, a decrease in the ΔD was observed in the QCM-D experiments. Typical we would expect the final layer of an LBL to be rather labile, but in this instance the results suggest that the heparin essentially locks the LBL structure into place once absorbed, creating a dense, rigid layer. The AFM data of the LBL 7 system with and without heparin strengthens this hypothesis. For the LBL 7 coating, it appears that the layer thickness is such that once it is dried for AFM analysis, it collapses in a more heterogeneous manner compared to the LBL 5 coating, resulting in the large protrusions observed in Figure 4C. However, if heparin is absorbed before either system is dried, then the AFM image looks very similar. The high resolution N 1s data suggests that the heparin complexes with the LBL coating with the component associated with charged N species (Figure 3B, C2) remains at approximately 50% compared to the coating without heparin. The interaction would thereby occur between the acid groups of the heparin and the basic groups of the PEI.

Assuming a uniform layer of heparin within the XPS sampling region, the thickness (x) of the heparin layer on the Si coated wafer was calculated using a standard XPS overlayer algorithm:⁴¹

$$I = I_{\infty} (1 - e^{-x/(\lambda \sin \theta)}) \quad (1)$$

where I is the intensity of the peak of interest (S in this case), I_{∞} corresponds to the same peak but from an infinitely thick film (i.e. the theoretical amount of S in heparin), λ_r is the attenuation length for the element in question and θ is the take off angle. For the LBL 5 system on Si, the heparin layer was calculated at 1.56 nm thick while on the LBL 7 system was 1.69 nm. High levels of S were also detected for the two scaffolds employed (on PP: S ~ 2.8 %; on PLGA ~ 3.1%). These values of S are significant when compared to that reported previously; for example, S < 0.6% absorbed onto plasma polymerized allylamine,⁴² S = 0.7% absorbed onto PEG grafted films,⁴³ S = 1.27% covalently coupled to poly(DL-lactic acid),⁴⁴ S = 3.22% covalently coupled to glycidyl methacrylate.⁴⁵ As outlined previously, attempts to maintain a regulated release of bioactive growth factors to a wound site via an angiogenic biomaterial

have not been very successful to date due to issues associated with rapid loss of heparin. Thus, the ability to immobilize such a large amount of heparin in a non-covalent manner, thereby maintaining functionality, is certainly promising. It is worth noting that work using chemical gradients of plasma polymerized allylamine have suggested that a high level of heparin does not translate to a high level of biological functionality.⁴⁶ However, the surfaces explored here are chemically and physically very different to the directly grafted heparin films, with significantly more heparin attached to the surface. As such, it is not practical to extrapolate results from that system to the current research, though it does provide avenues for future work exploring the amount of heparin absorbed vs. the biological angiogenic activity of this coating.

To examine the translation of the coating into a cellular environment, two scaffolds were chosen, a clinically used polypropylene mesh used for hernia and prolapse repair,^{24, 25} and a biodegradable PLGA scaffold being developed for wound repair.²⁶ XPS analysis illustrated that both of these materials could be successfully functionalized to bear heparin using the plasma polymer/LBL system. ELISA data shows VEGF associated equally with the 3, 5 and 7 LBL scaffolds, in the light of the relative instability of heparin binding to the 3 and 5 layer LBL surfaces, only the 7 layer LBL heparin was considered to be suitable for further cell attachment. The LBL system immobilises heparin by electrostatic attraction created by the successive layers bearing opposite charge; thus it is possible that the 7 layer system provides a greater electrostatic attraction for the immobilisation of heparin giving increased stability relative to the 5 and 3 layer surfaces.

Cell attachment experiments illustrated that while the heparin reduced the overall attachment of cells to the scaffold, adhesion being reduced to sparse single cells, once VEGF was added to the heparin surface, there were visible clusters of cells. Whether this was due to increased adhesion of cells in areas where heparin was absent, or where heparin-VEGF moieties were clustered, or cell proliferation promoted by VEGF -we cannot say. Further experimentation to identify the distribution of heparin and heparin-VEGF would be required. In the scaffolds lacking both heparin and VEGF, there was visibly more adhesion of cells overall - but these were single cells or small 2-3 cell clusters perhaps indicating good adhesion but little proliferation in contrast to samples where VEGF was used.

It is not unusual that the heparin coated surfaces failed to induce cell attachment. It has been shown that some cell types can be inhibited as a result of sugars like dextran and heparin binding to fibronectin or collagen.⁴⁷⁻⁵² In this study, when VEGF was added to the heparin-coated scaffold, HDMEC cells appeared to form colonies when seeded directly onto the scaffold or when allowed to migrate onto the scaffold. VEGF has been shown to be bioactive⁴ both while bound to extracellular matrix, and released from the ECM. There is also evidence showing VEGF bound covalently to hydrogels promoting proliferation, migration, and angiogenesis.^{53, 54} In scaffolds bearing heparin or heparin-VEGF there can be a promotion of cell ingrowth and vasculogenesis *in vivo* and influence regeneration of tissue^{55, 56} Therefore although our heparin/VEGF coated scaffold may not initially attract and allow adhesion of as many cells as the bare scaffold, these results clearly indicate that the presence of VEGF bound to heparin promoted increased numbers of cells.

Conclusions

The treatment of chronic wounds and the ultimate success of tissue grafted to a patient rely on the timely development of new vasculature to support healing a new tissue – failure to vascularize is a major cause of skin graft failure. Heparin and other proteoglycans found in the extracellular matrix are able to sequester growth factors and present them in a bound but active form, while VEGF is able to bind to heparin and promote vasculogenesis and proliferation of HDMEC cells. This study presents a novel application for the creation of heparin surfaces on flexible scaffolds to promote angiogenesis by sequestering VEGF to promote proliferation and migration of vascular endothelial cells. A coating strategy based on plasma phase deposition and LBL chemistry was successfully developed. QCM-D was employed to monitor and provide insight into the deposition kinetics of the coating process and the ability of the final coating to adsorb heparin. XPS analysis of the S content of the films (3.0 % for LBL 7 layer vs. 2.8 % for LBL 5) confirmed the trend observed via QCM-D. While differences were observed in the morphology between the LBL 5 and LBL 7 systems, once heparin was absorbed both surfaces appeared similar; together with the QCM-D data, the results suggested that the absorbed heparin locked the film structure into place thus preventing changes in the film morphology during the drying process. The coating methodology was successfully transferred to two tissue scaffold architectures, a commercially available non-biodegradable polypropylene mesh and a biodegradable electrospun PLGA scaffold reported previously. Compared to the LBL films on Si, the elemental composition of the coatings on the scaffolds was marginally different (O/N ~ 1:1 vs. ~ 1.1:1), while the high resolution C 1s profile suggested minimal difference in chemical functionality, and heparin retention. *In vitro* data shows that while HDMEC cells could readily attach to the uncoated and LBL 7 coated scaffold, they did not appear to form colonies and showed limited proliferation. While the immobilization of heparin to the scaffold surfaces reduced cell attachment, the addition of VEGF increased cell number, indicating that the bound VEGF was active and able to promote proliferation of the HDMEC cells. The results of this study clearly demonstrate the development of versatile methodology for functionalizing scaffolds with heparin for the fabrication of angiogenic biomaterials. This ability is highly desirable in the promotion of angiogenesis in both chronic wounds and in the creation of tissue engineered constructs to facilitate engraftment in a recipient.

Acknowledgements

We thank Dr Silvia Marchesan and Dr Thomas Gengenbach for useful discussions. We gratefully acknowledge support for Prof S MacNeil from the Royal Academy of Engineering to undertake a sabbatical visit to IRIS to initiate this research.

Notes and references

^a CSIRO Materials Science and Engineering, Bayview Avenue, Clayton VIC 3168, Australia.

^b Department of Engineering Materials, University of Sheffield, Kroto Research Institute, Broad Lane, Sheffield, S3 7HQ, UK.

^c Biotactical Engineering Group, IRIS, Faculty of Engineering and Industrial Sciences, Swinburne University of Technology, Hawthorn, Victoria 3122, Australia.

- N. Ferrara, H. Chen, T. Davis-Smyth, H. P. Gerber, T. N. Nguyen, D. Peers, V. Chisholm, K. J. Hillan and R. H. Schwall, *Nat. Med.*, 1998, 4, 336-340.
- L. Gilmore, S. Rimmer, S. L. McArthur, S. Mittar, D. Sun and S. MacNeil, *Biotechnology and Bioengineering*, 2013, 110, 296-317.
- K. A. Houck, D. W. Leung, A. M. Rowland, J. Winer and N. Ferrara, *J. Biol. Chem.*, 1992, 267, 26031-26037.
- J. E. Park, G. A. Keller and N. Ferrara, *Mol. Biol. Cell*, 1993, 4, 1317-1326.
- A. Zieris, K. Chwalek, S. Prokoph, K. R. Levental, P. B. Welzel, U. Freudenberg and C. Werner, *J. Control. Release*, 2011, 156, 28-36.
- Y. Huang, L. Taylor, Chen X., and N. Ayres, *Polymer Chemistry*, 2013, 51, 5230.
- L. Taylor, X. Chen, and N. Ayres, *Polymer International*, 2014, 63, 127.
- S. Singh, B. M. Wu and J. C. Y. Dunn, *Biomaterials*, 2011, 32, 2059-2069.
- J. J. Yoon, H. J. Chung, H. J. Lee and T. G. Park, *J. Biomed. Mater. Res. Part A*, 2006, 79A, 934-942.
- A. Lode, A. Reinstorf, A. Bernhardt, C. Wolf-Brandstetter, U. Konig and M. Gelinsky, *J. Biomed. Mater. Res. Part A*, 2008, 86A, 749-759.
- G. C. M. Steffens, C. Yao, P. Prevel, M. Markowicz, P. Schenck, E. M. Noah and N. Pallua, *Tissue Eng.*, 2004, 10, 1502-1509.
- B. Demirdogen, A. E. Elcin and Y. M. Elcin, *Growth Factors*, 2010, 28, 426-436.
- H. J. Chung, H. K. Kim, J. J. Yoon and T. G. Park, *Pharm. Res.*, 2006, 23, 1835-1841.
- D. W. Tang, S. H. Yu, Y. C. Ho, F. L. Mi, P. L. Kuo and H. W. Sung, *Biomaterials*, 2010, 31, 9320-9332.
- S. MacNeil, *Nature*, 2007, 445, 874-880.
- G. Decher, *Science*, 1997, 277, 1232-1237.
- W.-B. Tsai, R. P.-Y. Chen, K.-L. Wei, Y.-R. Chen, T.-Y. Liao, H.-L. Liu and J.-Y. Lai, *Acta Biomaterialia*, 2009, 5, 3467-3477.
- Q. K. Lin, J. J. Van, F. Y. Qiu, X. X. Song, G. S. Fu and J. A. Ji, *J. Biomed. Mater. Res. Part A*, 2011, 96A, 132-141.
- M. Lundin, E. Blomberg and R. D. Tilton, *Langmuir*, 2010, 26, 3242-3251.
- M. S. Niepel, D. Peschel, X. Sisquella, J. A. Planell and T. Groth, *Biomaterials*, 2009, 30, 4939-4947.
- T. G. Kim, H. Lee, Y. Jang and T. G. Park, *Biomacromolecules*, 2009, 10, 1532-1539.
- Q. G. Tan, J. Ji, M. A. Barbosa, C. Fonseca and J. C. Shen, *Biomaterials*, 2003, 24, 4699-4705.
- Z. W. Mao, L. Ma, J. Zhou, C. Y. Gao and J. C. Shen, *Bioconjugate Chem.*, 2005, 16, 1316-1322.
- J. C. Winters, M. P. Fitzgerald and M. D. Barber, *BJU Int.*, 2006, 98, 70-76.
- M. E. Karlovsky, A. A. Thakre, A. Rastinehad, L. Kushner and G. H. Badlani, *Urology*, 2005, 66, 469-475.
- K. A. Blackwood, R. McKean, I. Canton, C. O. Freeman, K. L. Franklin, D. Cole, I. Brook, P. Farthing, S. Rimmer, J. W. Haycock, A. J. Ryan and S. MacNeil, *Biomaterials*, 2008, 29, 3091-3104.
- M. Salim, P. C. Wright and S. L. McArthur, *Electrophoresis*, 2009, 30, 1877-1887.
- T. R. Gengenbach and H. J. Griesser, *J. Polym. Sci. Pol. Chem.*, 1998, 36, 985-1000.
- M. Rodahl, Hook, F., Krozer, A., Brzezinski, P., Kasemo, B., *Rev. Sci. Instrum.*, 1995, 66, 3924-3930.
- K. Gupta, S. Ramakrishnan, P. V. Browne, A. Solovey and R. P. Hebbel, *Exp. Cell Res.*, 1997, 230, 244-251.
- M. Cantini, P. Rico, D. Moratal and M. Salmeron-Sanchez, *Soft Matter*, 2012, 8, 5575-5584.
- S. Marchesan, C. D. Easton, K. E. Styan, P. Leech, T. R. Gengenbach, J. S. Forsythe and P. G. Hartley, *Colloid Surf. B-Biointerfaces*, 2013, 108, 313-321.
- M. Muller, B. Kessler, N. Houbenov, K. Bohata, Z. Pientka and E. Brynda, *Biomacromolecules*, 2006, 7, 1285-1294.
- M. Elzbieciak, M. Kolasinska, S. Zapotoczny, R. Krastev, M. Nowakowska and P. Warszynski, *Colloid Surf. A-Physicochem. Eng. Asp.*, 2009, 343, 89-95.

35. G. M. Liu, J. P. Zhao, Q. Y. Sun and G. Z. Zhang, *J. Phys. Chem. B*, 2008, 112, 3333-3338.
36. M. Müller, T. Rieser, K. Lunkwitz, S. Berwald, J. Meier-Haack and D. Jehnichen, *Macromolecular Rapid Communications*, 1998, 19, 333-336.
37. M. Muller, T. Rieser, P. L. Dubin and K. Lunkwitz, *Macromolecular Rapid Communications*, 2001, 22, 390-395.
38. L. Shen, B. Wang, J. Wang, J. Fu, C. Picart and J. Ji, *ACS Applied Materials & Interfaces*, 2012, 4, 4476-4483.
39. B. Schoeler, E. Poptoshev and F. Caruso, *Macromolecules*, 2003, 36, 5258-5264.
40. D. Kovacevic, S. van der Burgh, A. de Keizer and M. A. C. Stuart, *Langmuir*, 2002, 18, 5607-5612.
41. D. F. Mitchell, K. B. Clark, J. A. Bardwell, W. N. Lennard, G. R. Massoumi and I. V. Mitchell, *Surf. Interface Anal.*, 1994, 21, 44-50.
42. D. E. Robinson, D. J. Buttle, R. D. Short, S. L. McArthur, D. A. Steele and J. D. Whittle, *Biomaterials*, 2012, 33, 1007-1016.
43. K. N. Pandiyaraj, V. Selvarajan, Y. H. Rhee, H. W. Kim and S. I. Shah, *Mater. Sci. Eng. C-Biomimetic Supramol. Syst.*, 2009, 29, 796-805.
44. T. Sharkawi, V. Darcos and M. Vert, *J. Biomed. Mater. Res. Part A*, 2011, 98A, 80-87.
45. Y. S. Chen and P. Liu, *J. Appl. Polym. Sci.*, 2004, 93, 2014-2018.
46. D. E. Robinson, A. Marson, R. D. Short, D. J. Buttle, A. J. Day, K. L. Parry, M. Wiles, P. Highfield, A. Mistry and J. D. Whittle, *Adv. Mater.*, 2008, 20, 1166-+.
47. C. Mendes de Aguiar, B. Lobao-Soares, M. Alvarez-Silva and A. Trentin, *BMC Cell Biology*, 2005, 6, 31.
48. J. Laterra, J. E. Silbert and L. A. Culp, *J. Cell Biol.*, 1983, 96, 112-123.
49. M. Mochizuki, N. Yamagata, D. Philp, K. Hozumi, T. Watanabe, Y. Kikkawa, Y. Kadoya, H. K. Kleinman and M. Nomizu, *Biopolymers*, 2007, 88, 122-130.
50. T. Weiss, S. Ricard-Blum, L. Moschovich, E. Wineman, S. Mesilaty and E. Kessler, *J. Biol. Chem.*, 2010, 285, 33867-33874.
51. R. J. Klebe and P. J. Mock, *J. Cell. Physiol.*, 1982, 112, 5-9.
52. J. D. Sanantonio, A. D. Lander, T. C. Wright and M. J. Karnovsky, *J. Cell. Physiol.*, 1992, 150, 8-16.
53. A. M. Porter, C. M. Klinge and A. S. Gobin, *Biomacromolecules*, 2011, 12, 242-246.
54. A. M. Porter, C. M. Klinge and A. S. Gobin, *Am. J. Physiol.-Cell Physiol.*, 2011, 301, C1086-C1092.
55. K. M. Brouwer, R. M. Wijnen, D. Reijnen, T. G. Hafmans, W. F. Daamen, and T. H. van Kuppevelt, *Organogenesis.*, 2013, 9, 161.
56. S. Knaack, A. Lode, B. Hoyer, A. Rosen-Wolff, A. Gabrielyan, I. Roeder, and M. Gelinsky, *J. Biomed. Mater. Res. A*, 2013, doi: 10.1002/jbm.a.35020.